Oedometer test contribution for the Study of deformation in oil reservoirs

Ribeiro, João Filipe
Email addresses: joaoamadoribeiro@ist.utl.pt
Instituto Superior Técnico
Avenida Rovisco Pais, 1
1049-001 Lisboa

Abstract. The fluid production in an oil reservoir induces variations of the pressures that can affect the stress state and cause deformation on reservoir rock and affect the surrounding rocks. The evaluation of the reservoir rocks compressibility plays an important role because it allows us to obtaining a prediction of reservoir deformation by pressure change; thereby it allows minimizing adverse effects associated with this phenomenon.

In this study oedometer tests were carried out on a rock with reservoir potential subjected to a vertical load in order to evaluate its compressibility. It is the best experimental test to reproduce the reservoir conditions and their response to the increase of effective stress in response to reservoir depletion.

Through application of commercial software Plaxis, which is based on finite element method, it has created a computer simulation of oedometer test and evaluated the adequacy of its use when compared with experimental test results.

To achieve the objectives of this work the results of deformability obtained by oedometer test was compared to a real gas field deformability data.

1. Introduction

The subsidence caused by groundwater extraction, oil and gas has been observed and studied for over a hundred years. Some of the earliest known examples of subsidence due to groundwater extraction are: London, England (first noted in 1865), Osaka, Japan (first noted in 1885), and Mexico City, Mexico (referred to for the first time 1929) (Leonid F. Khilyuk, 2000).

The compaction phenomenon is to the volume reduction of a reservoir rock due to its compression, which leads to a decreasing of reservoir thickness, especially where the production wells are located. The reservoir deformation can lead to a movement of overlying layers until surface - subsidence (Figure 1).

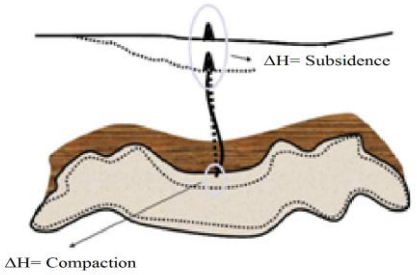

Figure 1 Compaction and subsidence.

Generally oil or gas reservoirs undergo compaction, but in most situations this value is greatly reduced, so the subsidence of the surface is negligible. However this phenomenon is one of main concern in oil industry because it can be responsible for significant environmental impacts with respect to increased risks of flooding on terrestrial operations know by the case Long Beach in California (Mayuga, 1970); Bolivar Cost in Venezuela (Finol & Sancevic, 1995); Ravenna in Italia (Teatini, et al., 2005), or the worsening security of offshore production platforms, as noted in the Ekofisk oilfield in the North Sea (Pemper, et al., 1998).

On the other hand compression of the oil reservoir can result in excessive deformation of the well casing and therefore be responsible for serious operational problems related to the hydrocarbons production.

2. Objectives

This work contributes for the discussion of the appropriateness of laboratory tests, as oedometer test used in order to study the compression phenomenon on reservoirs.

In this dissertation, the study of compression phenomenon is based by use of the test oedometer on a saturated limestone specimen with drained conditions in order to assess the deformations along the loading time and according to various loads.

Through application of Plaxis is intended to create a computer simulation of oedometer test and compare the results obtained experimentally.

3. Mechanisms responsible for compaction and subsidence

Fluid extraction (water, gas or oil) from a petroleum reservoir results in reduction of pore pressure and consequently increase of effective stress in a porous rock.

The pore pressure decrease leads to changes in the stress state at the reservoir level that not only induce compaction and subsidence, but can also lead to changes in fluid flow performance. The permeability may be changed as well as the directions of preferential paths of fluid within the reservoir.

Dake (1978) supports that the reservoir compression, as well as the effect of surface subsidence will be more pronounced in shallow reservoirs (<1000 meters) with high porosity than reservoirs constituted by competent and deeper sandstones.

3. Compaction Fundamentals

The compaction phenomenon described by Terzaghi in 1943 to a porous media subjected to a constant vertical load. This problem can be characterized by a permeable porous rock saturated with water, with length, h and large width on a rigid and impermeable backing submitted to a vertical load (Figure 3.1) (Gomes, 2009)

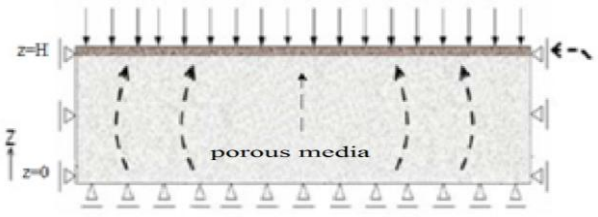

Figure 2 Geometry for a compression problem.

According the Terzaghi principle the saturated soil compression is studied admitting that to part of the applied load is distributed to the solid skeleton, σ'_v and supported by water, p (pore pressure).

Excluding purely thermal effects or chemical effect, such as dissolving, compressing a reservoir is governed by three primary parameters:

- $\Delta\sigma'_v$ change in the vertical effective stress;

- c_b Reservoir compressibility;

- H Reservoir thickness.

The reservoir thicknesses as well as the compressibility of the reservoir rock are intrinsic characteristics of the reservoir. In most cases, they cannot be altered or changed. However in certain reservoir rock compressibility can vary by three orders of magnitude so it´s one of the most difficult parameters to measure especially at the reservoir scale (Nagel, 2001)

In reservoir engineering the reservoir compaction along the vertical direction is generally characterized by the uniaxial compaction coefficient, c_m:

The total compaction of the reservoir ΔH for a given time depends on the pressure change, Δp from the production beginning as well as the reservoir height, H:

$$\Delta H = c_m . \Delta p . H \quad (1)$$

In order to analyze the influence of the effects of compression on a reservoir subsidence at the surface, there are some methods were developed. One of the most common methods for subsidence assessment is Nucleus of Strain method presented by Geertsma (1973).

Building upon this, Geertsma developed analytical equations called the Nucleus of Strain method, for estimating reservoir compaction and surface subsidence (Geertsrna, 1973). Equation (3) shows the basic formulation for subsidence from a nucleus of strain that Geertsma later extended to the case of a disc-shaped reservoir at some depth:

$$u_z(r,0) = -\frac{c_m(1-\nu)}{\pi\,(r^2+D^2)^{3/2}}\Delta P . V \quad (3)$$

Where $u_z(r,0)$represents surface subsidence at some arbitrary location a horizontal distance r from a point of compaction, $C_{m\ is}$ the uniaxial compaction coefficient $(Kg/cm^2)^{-1}$, ν is Poisson's ratio, ΔP is the reduction of the pore pressure (Kg/cm^2), D is the vertical depth from surface to the point of compaction and V is the *nucleus of strain* volume (Ketellar, 2009).

4. Experimental tests used to assess compaction

Among several experimental tests that determine the pore compressibility, the hydrostatic test and the oedometer test are the most used.

The hydrostatic test is often performed due its simplicity, speed and low cost. The test consists in obtaining the pore compressibility through the pore pressure change, or by change the confining pressure. However, this test is conducted under the same tension on all directions (hydrostatic stress) which does not represent the state of

stress in the reservoir or the effective stress change during production. So pedometer tests are more accepted (FJÆR, et al., 2008).

The oedometer test measures the pore pressure change per increment of axial stress where sides of the sample are prevent its lateral expansion.

It´s necessary to specify the method used to determine the rock compression. The pore elasticity theory shows that these two compressibility's can be related to each other:

$$\beta_1 = \frac{\alpha}{3}\frac{(1+\nu)}{(1-\nu)}\beta \quad (4)$$

Where, β_1 is rock axial compressibility measured by oedometer test, β is rock axial compressibility measured by hydrostatic test.

5. Oedometer test

The oedometer test proposed by Terzaghi consists of the application of increasing tension to a laterally confined specimen subjected to an axial load, in order to evaluate the settlements over time. Having regard to the lateral confinement, the lateral deformations ($\Delta\varepsilon_{lateral}$) are zero and deformation occurs only in the vertical direction ($\Delta\varepsilon_{Vertical}$) which corresponds to a volumetric strain ($\Delta\varepsilon_{Vol} = \Delta\varepsilon_{Vertical}$).

The specimen is saturated in order to simulate the behavior of rock iteration / water and is drained conditions (pressure constant pores) in order to represent change of effective stress in reservoir. During the test the water drains through the porous plates placed on the top and bottom of the specimen. According to BS 1733 standard it is assumed at least 24 hours between each tension increase. This waiting period is related to the time that pore pressure takes to be dissipated.

The deformations are calculated by:

$$\varepsilon = \frac{\Delta h}{h_i} = \frac{\Delta e}{1+e_i} \quad (5)$$

and

$$\Delta H = \frac{\Delta e}{1+e_i}.h_i = \Delta\sigma'.h_i.m_v \quad (6)$$

Where σ'_z – vertical effective stress;

$\Delta\sigma'$ – effective stress increment;

$\Delta\varepsilon_z$ – Vertical strain change;

Δh – Change in thickness specimen;

h_0 – Initial thickness of the specimen.

Thus, it´s possible to plot the test results graphically and obtain the trajectories being obtained by calculating the change in the void ratio from vertical displacement, since the volumetric strain corresponds to the vertical deflection as previously demonstrated.

The graph shown in Figure 3.7, allows to represents the variation of void ratio during loading applied in oedometer test.

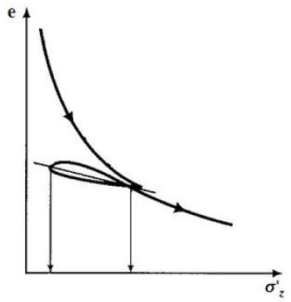

Figure 9 Void ratio with effective vertical stress.

Where,

$$m_v = -\frac{H_i - H_f}{H_i}\frac{1000}{\sigma'_{v2} - \sigma'_{v1}} = c_m \quad (7)$$

σ'_{v1} is the stress on specimen in the previous load increment (KPa), σ'_{v2} is the stress on specimen at the load increment to be considered (KPa), m_v is expressed in MPa^{-1}.

From oedometer test is also determined the oedometer modulus, E_{ed} (Bhuiyan, et al., 2012) is given by the relation (isotropic properties):

$$E_{ed} = \frac{\Delta\sigma_v}{\Delta\varepsilon_v} = E\frac{(1-\nu)}{(1-2\nu)(1+\nu)} \quad (9)$$

And the incremental stress confinement is given by:

$$K_0 = \frac{\Delta\sigma_h}{\Delta\sigma_v} = \frac{\upsilon}{1-\upsilon} \quad (10)$$

Where $\Delta\sigma_v$ e $\Delta\sigma_h$ is the change of vertical stress (axial) and horizontal (confinement) respectively and $\Delta\varepsilon_v$ is the specimen vertical strain.

6. Methodology

This chapter describes the case study as well as the methodology followed in order to evaluate the influence of the effective stress variation during hydrocarbon production cycle on reservoir strain. In this study, the

strain evaluation of the sample is made based on two aspects: computational methods and experimental methods. We intend to compare the results obtained with both methods.

Following the proposed objectives for this work, we selected a geological unit the study, whose characteristics are similar to carbonate reservoirs - Limestone from Codaçal (Figure 3). The limestone from Codaçal belongs to formation Santo Antonio in Serra de S. Bento (Narciso, 2014).

Figure 3 Specimen – Limestone from Codaçal.

Oedometer tests were performed in order to study the rock compressibility rock in accordance with BS 1733, Part 6, however we didn't measure pore pressures during the test. The tests considers only loading phase by analogy to the reservoirs compaction by pore pressure reducing.

The preparation of limestone from Codaçal samples consisted on cutting and smoothing the cylindrical surfaces in order to obtain a good fit between the specimen and the test equipment. Thus they were prepared six specimens with 63 mm diameter and 34 mm height. The determination of voids was made by weighing each sample after 24 hours in a drying oven, and weighed m_{dry} and then submerged over 48 hours in water, m_{sat}.

The specimen is stressed in accordance with the assumptions base on Terzaghi theory:

- The rock is saturated (submerged);

- The rock is confined (rigid ring);

- The flow is vertical (impermeable ring).

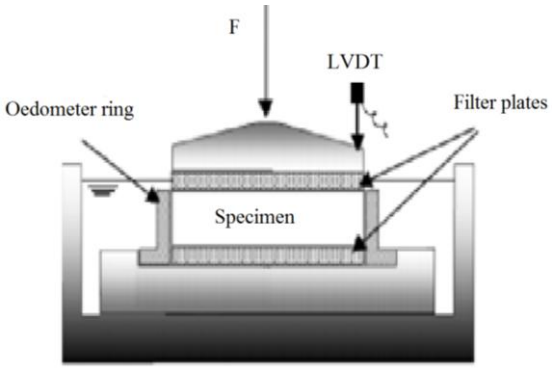

Figure 4 Oedometer test scheme.

Table 1 shows the loading plan with respective duration.

Table 1 Loading plan for oedometer test.

Load	Sample 1	Sample 2	Sample 3
1	1,88MPa	1,88MPa	1,88MPa
2	3,76MPa	3,76MPa	3,76MPa
3	7,52MPa	7,52MPa	7,52MPa
4	15,40MPa	15,40MPa	15,40MPa
5	30,08MPa	30,08MPa	30,08MPa

Load	Sample 4	Sample 5	Sample 6
1	1,88MPa	1,88MPa	7,52MPa
2	3,76MPa	3,76MPa	15,40MPa
3	7,52MPa	7,52MPa	30,08MPa
4	15,40MPa	15,40MPa	-
5	30,08MPa	30,08MPa	-

Equipment

The press (ELE) used in this study is in the Instituto Superior Técnico geomechanics laboratory.

The system is composed by a control unit with ability to control speed of loading.

Oedometer simulation

The model was designed by an extract with 34mm high and 63mm wide, just like samples tested in the laboratory. The boundary conditions and in order to represent the condition imposed on the specimen was considered mobile supports laterally, which only allow vertical displacements. On the bottom the model considers fixed supports which prevent displacement in any direction, as represented in Figure 5.

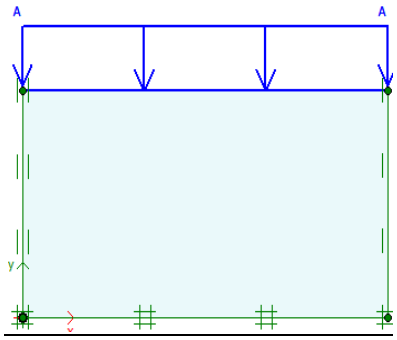

Figure 5 Schematic representations of boundary conditions

The finite element mesh adopted is composed by triangular elements with 15 nodes. This mesh is represented in Figure 12 and it was automatically generated by the software.

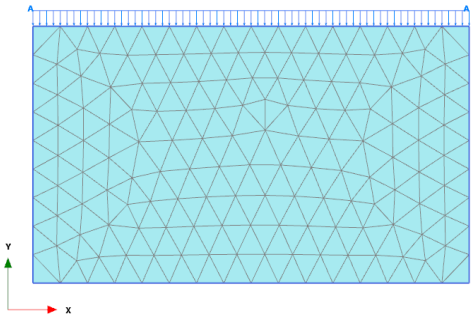

Figure 6 Mesh adopted and representation of load.

Rock properties

The Poisson ratio adopted was based on the study by Narciso (2014) that study the same limestone. The values obtained from Narcissus (2014) range between 0.22 and 0.30. So, in this study opted 0.25 for Poisson ration. The module of elasticity, and was determined from the oedometer elasticity module, E_{oed} experimentally determined through oedometer test and the relationship between the two parameters described in the Plaxis manual:

$$E_{ed} = \frac{(1-\nu)E}{(1-2\nu)(1+\nu)} \qquad (11)$$

7. Results and discussion

Case study – Groningen reservoir

To analyze the problem, it was taken as the reference gas field Groningen presented by Castro, et al. (2005) and Nederlandse Aardolie Maatschappij (2013).

The use of Groningen gas field in this study is due to the available information of data field from the reservoir.

Doorhof, et al. (2006) provides the measurements obtained by monitoring the induced subsidence, i.e. only due reservoir depletion, and reservoir compaction along the production.

There is an almost linear relationship between subsidence and reservoir compaction.

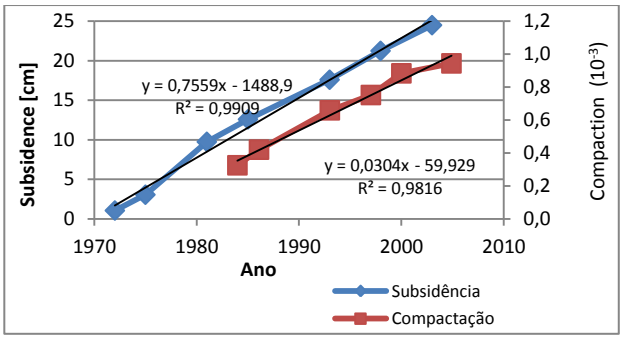

Figure 7 Compaction and subsidence versus time - Groningen reservoir.

Uniaxial compaction coefficient

It is intended in this section discuss the representatively of oedometer test on evaluation of reservoir compaction of Groningen.

In Doorhof, et al. (2006) is graphically displayed the relationship between subsidence measurement on surface with the measurement of pore pressure within the reservoir (Figure 8). We established a trend line showing a linear relationship given by the equation in Figure 8 .

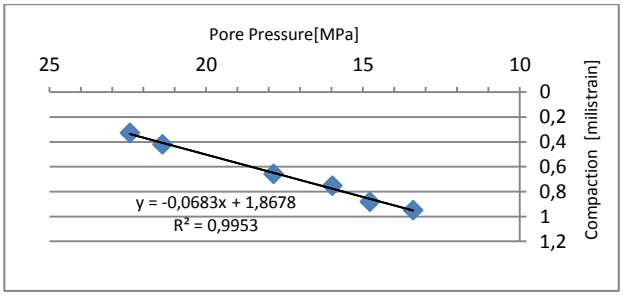

Figure 8 Pore pressure versus reservoir compaction (Groningen field).

The uniaxial compression ratio in situ, m_v observed in situ is obtained from the slope of the linear regression from the graph in Figure 5.2 where $m_v = 6{,}83x10^{-5}MPa^{-1}$.

In Doorhof, et al. (2006) oedometer tests were also carried out to assess the compressibility of the reservoir. The tests were carried out on 5 reservoir samples where there was obtained $m_v=6{,}0x10^{-5}MPa^{-1}$ for a range loads between 33 and 10 MPa. There is thus a good approximation between the results of oedometer test and data obtained within reservoir.

Oedometer test

We present the results obtained in oedometer test in order to determine the compressibility of the Limestone from Codaçal.

In Figure 9 are presented the results of void ration due effective stress on logarithmic scale for the samples.

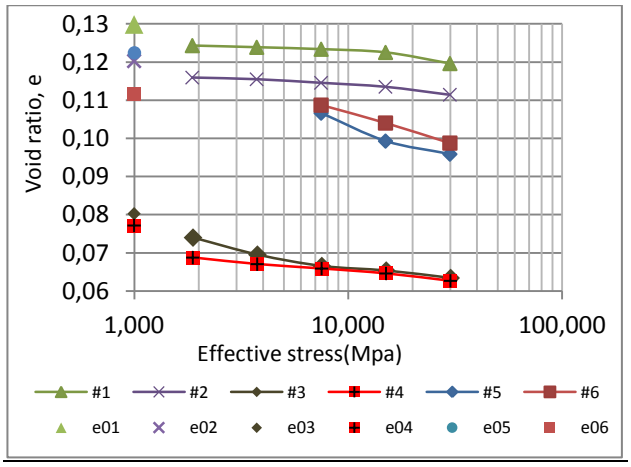

Figure 9 Void ratio versus effective stress obtained from oedometer test. e_0 is the initial void ratio for each sample.

The BS 1377 provides graphic presentation of displacement versus time for each load level. Figure 10 presents the settlements for each load level.

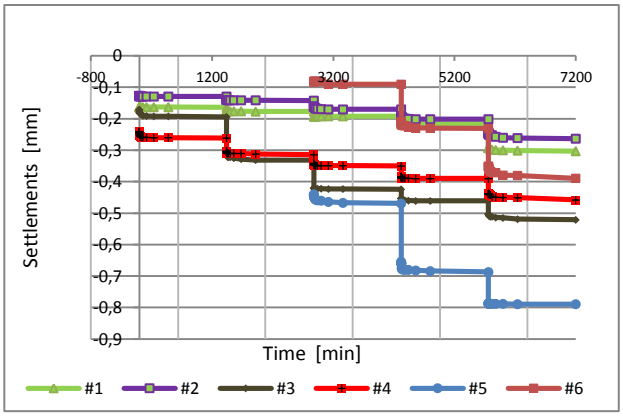

Figure 10 Axial settlements for each load level (1,88MPa, 3,76MPa, 7,52MPa, 15,40MPa, 30,084MPa)

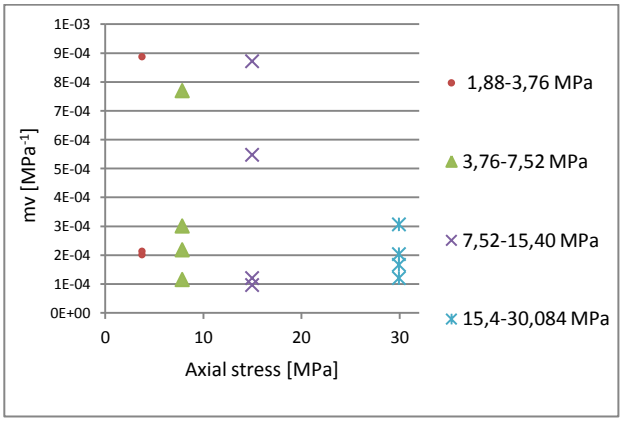

Figure 11 Uniaxial compaction coefficient for specimens for load level.

Comparison of numerical simulation and oedometer test results

For of E_{ed} analysis and subsequent comparison with same parameter obtained by numerical simulation we considered the loads from the first load step (1880KPa or 752KPa) applied in oedometer test up to the last load step (3080 kPa).

Specimen 1

The parameters selected from Mohr-Coulomb model, for sample 1 in Table are given by Table 2.

Table 2 Mohr-Coulomb Input parameters – Numerical simulation of oedometer test - specimen 1.

E_{ed} [KN/m2]	ν
$6{,}957x10^{6}$	0,25

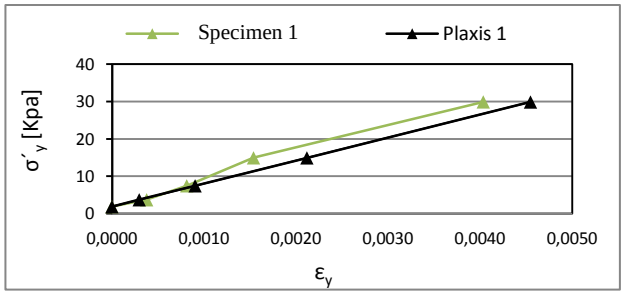

Figure 12 Curve Stress/Strain of oedometer test and Plaxis simulation – Specimen 1.

Specimen 2

The parameters selected from Mohr-Coulomb model, for sample 2 in Table are given by Table 3.

Table 3 Mohr-Coulomb Input parameters – Numerical simulation of oedometer test - specimen 2.

E_{ed} [KN/m2]	*v*
$7{,}140 \times 10^6$	0,25

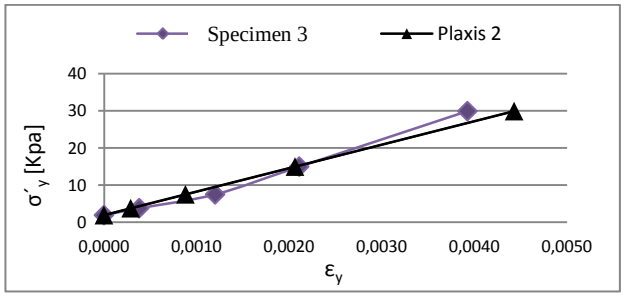

Figure 13 Curve Stress/Strain of oedometer test and Plaxis simulation – Specimen 2.

Specimen 3

The parameters selected from Mohr-Coulomb model, for sample 2 in Table are given by Table 4.

Table 4 Mohr-Coulomb Input parameters – Numerical simulation of oedometer test - specimen 3.

E_{ed} [KN/m2]	*v*
$2{,}739 \times 10^6$	0,25

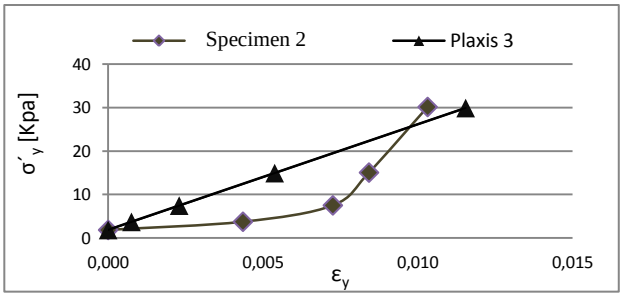

Figure 14 Curve Stress/Strain of oedometer test and Plaxis simulation – Specimen 3.

Specimen 4

The parameters selected from Mohr-Coulomb model, for sample 4 in Table are given by Table 5.

Table 5 Mohr-Coulomb Input parameters – Numerical simulation of oedometer test - specimen 4.

E_{ed} [KN/m2]	*v*
$4{,}546 \times 10^6$	0,25

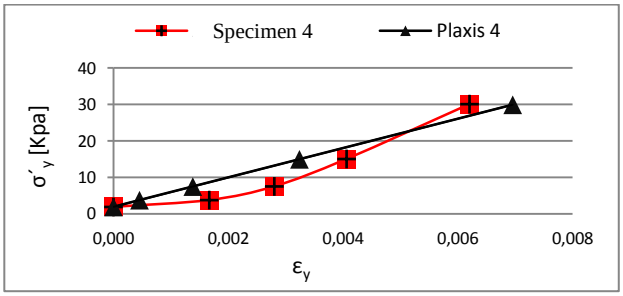

Figure 15 Curve Stress/Strain of oedometer test and Plaxis simulation – Specimen 4.

Specimen 5

The parameters selected from Mohr-Coulomb model, for sample 5 in Table are given by Table 6.

Table 6 Mohr-Coulomb Input parameters – Numerical simulation of oedometer test - specimen 5.

E_{ed} [KN/m2]	*v*
$2{,}344 \times 10^6$	0,25

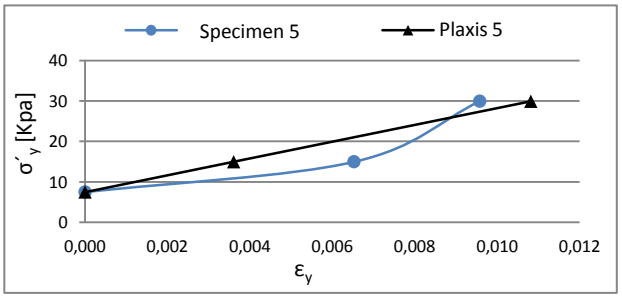

Figure 19 Curve Stress/Strain of oedometer test and Plaxis simulation – Specimen 5.

Specimen 6

The parameters selected from Mohr-Coulomb model, for sample 6 in Table are given by Table 7.

Table 7 Mohr-Coulomb Input parameters – Numerical simulation of oedometer test - specimen 6.

E_{ed} [KN/m2]	*v*
$2{,}58x10^{6}$	0,25

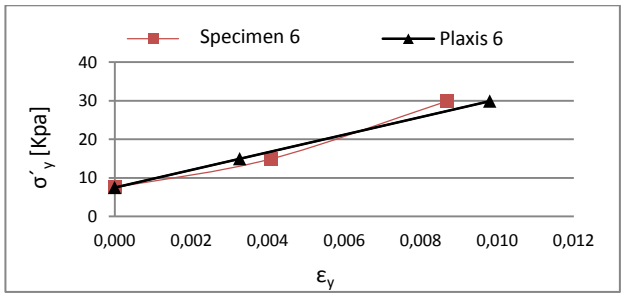

Figure 16 Curve Stress/Strain of oedometer test and Plaxis simulation – Specimen 6.

8. Conclusions

The work had as main objective study the suitability the application of laboratory tests in studies of compaction and subsidence phenomenon oilfield. Thereby a literature research was carried out in order to understand what limitations the various laboratory tests had when extrapolated to a reservoir scale.

Despite the subsidence phenomenon that this is subject of many studies, the information is very restricted, lacking available information data monitored in oil fields.

In the case study, it was found a good agreement between c_m for reservoir, 6,8x10-5 MPa-1 and the values obtained by oedometer from samples 6x10-5 MPa^{-1}**.** It is considered well demonstrated the importance of oedometer tests on samples when calculating the reservoir uniaxial compaction coefficient.

For the laboratory testing conducted in this study it is concluded that:

– The c_m obtained are in agreement with the values found in the bibliography;

– It was possible to simulate oedometer test by numerical simulation in Plaxis 2D, where was observed good agreements between results. Thus the Mohr-Coulomb constitutive model is capable to reproduce a good adjustment with experimental results.

– It was not possible to take better conclusions due to the restrict access of petroleum reservoir data.

10. REFERENCES.

Bhuiyan, M. H. et al., 2012. Static and dynamic behaviour of compacted sand and clay: Comparison between measurements in Triaxial and Oedometric test systems. *European Association of Geoscientits & Engineers*, December.

Doornhof, D. et al., 2006. Compaction and Subsidence. pp. 50-68.

Finol, A. S. & Sancevic, Z. A., 1995. Subsidence in Venezuela, Subsidence Due To Fluid Witlidrawl. *Elsevier Developments in Petroleum Science*, p. 337–372.

FJÆR, E. et al., 2008. *PETROLEUM RELATED ROCK MECHANICS.* 2nd EDITION ed. s.l.:s.n.

Fredrich, J., Arguello, J., Deitrick, G. & Rouffignac, E. d., 2000. Geomechanical Modeling of Reservoir Compaction, Surface Subsidence, and Casing Damage at the Belridge Diatomite Field. *SPE Reservoir Eval. & Eng. 3 (4)*, August.

Geertsma, J., 1973. Land Subsidence Above Compacting Oil and Gas Reservoirs. *Journal of Petroleum Technology*.

Gomes, I. F., 2009. *Implementação em elementos finitos das equações de pressão e saturação para simulação de fluxo bifásico em reservatórios de petróleo deformáveis.* Universidade Federal de Pernambuco - UFPE: Centro de Tecnologia e Geociências - CTG.

Ketellar, V. B. H., 2009. *Satellite Radar Interferometry - Subsidence Monitoring Techniques.* s.l.:Springer.

Mayuga, M., 1970. Geology and Development of California's Giant - Wilmington Oil Field. *American Association of Petroleum Geologists*, pp. 158-184.

Nagel, N. B., 2001. Compaction and Subsidence Issues Within the Petroleum Industry: From Wilmington to

Ekofisk and Beyond. *Phys. Chem. Earth (A), Vol. 26*, *Elsevier Science Ltd*, pp. 3-14.

Narciso, J. M. F., 2014. *Previsão e modelação de pressao de poros utilizando velocidades sísmicas*, Instituto Superior Técnico: Dissertação para obtenção do grau mestre em Engenharia de Petróleos.

Pemper, R., Gold, R. & Nagel, N. B., 1998. Monitoring Formation Compaction. *Baker Hughes*, pp. 22-33.

Pruiksma, J. P., Breunese, J. N., Visser, K. v. T. -. & Waal, J. A. d., 2015. Isotach formulation of the rate type compaction model for sandstone. *International Journal of Rock Mechanics & Mining Sciences - Elsevier*, June.

Teatini, P. et al., 2005. A century of land subsidence in Ravenna. *Italy*. *Environmental Geology 47*, pp. 831-846.